Basic Comprehension of a Flux-Driven Josephson Parametric Amplifier

Minsu Ko

Korea Advanced Institute of Science and Technology, Department of Physics

Institute for Basic Science, Center for Axion and Precision Physics Research

1 Josephson Parametric Amplifier

The Josephson Parametric Amplifier (JPA) is one of the quantum-noise-limited amplifiers widely used for low noise signal readouts, from axion haloscopes [1] to quantum computers [2]. Especially for axion haloscopes, JPAs are used as the first stage amplifiers right after a cavity since the total system noise is mainly determined by the noise temperature of the first stage amplifier of the system. Moreover, the resonance tunability of JPAs enables the combination of JPAs with tunable cavities. As a quantized circuit element, a modern theoretical model of the JPA [3] is not that simple. Nevertheless, it is possible to describe their overall features by harmonically combining basic concepts from classical mechanics, circuit theory, and quantum mechanics. In this section, I provide a theoretical comprehension of JPAs, including their resonance tunability, gain, noise, and the principle of signal amplification.

1.1 DC SQUID

A DC SQUID is the most important component inside a JPA. It makes the resonant frequency of the JPA tunable, and opens a way to exploiting the parametric amplification. The DC SQUID is a loop consisting of two Josephson junctions. I start with explaining the physics of Josephson junctions and how it is applied to the DC SQUID.

1.1.1 Josephson Junction

A Josephson junction is a weak link, or a small gap working as a superconducting tunnel between two superconductors. A significant feature of the Josephson junction is that a Cooper pair, not only a single electron, can flow through the weak link via quantum tunneling effect without power dissipation. A Josephson junction has its own critical current I_s, the maximum current flowing across the junction without voltage drop (power dissipation). An important characteristic of the weak link is that the phase gradient $\nabla\theta$ of an electron wave function is quite large compared to the phase gradients inside the superconductors. Especially for a tunnel junction, usually phase difference $\varphi = \theta_2 - \theta_1$ is used instead of the gradient. I will show that the relation between the current flowing through the Josephson junction I_s and the phase difference φ across it.

Consider the Schrödinger equation of the system with a discrete wave function basis expansion $\Psi(t) = \sum_\alpha C_\alpha(t)\psi_\alpha$.

$$i\hbar\frac{dC_\beta}{dt} = \sum_\alpha H_{\beta\alpha}C_\alpha(t) \tag{1.1}$$

Note that H_{ii} is the energy of the system in the state ψ_i and H_{ij} is representing the transition probability between two states ψ_i and ψ_j. Now assume that the current through the Josephson junction is so larger ($I_s > I_c$)that there is voltage V across the junction. Here I introduce the Feynman's approach [4]: we consider a system of Cooper pairs as a two-level quantum mechanical system. That is, an electron pair (with charge $2e$) can occupy either level 1 or 2, with corresponding energy H_{11} and H_{22}. Since there is a voltage V across the junction, we can easily set $H_{11} = +eV$ and $H_{22} = -eV$. Also, introducing the transition element $H_{12} = H_{21} = K$, a system of differential equations associated with the Hamiltonian is established.

$$H = \begin{pmatrix} eV & K \\ K & -eV \end{pmatrix} \tag{1.2}$$

$$\begin{cases} i\hbar\dfrac{dC_1}{dt} = eVC_1(t) + KC_2(t) \\ i\hbar\dfrac{dC_2}{dt} = KC_1(t) - eVC_2(t) \end{cases} \tag{1.3}$$

Provided that C_1 is the amplitude of the pair state at level 1, a physical interpretation forces one to set $|C_1|^2 = n_s$, where n_s is the density of superconducting electrons in the junction electrodes. For simplicity, assuming that both electrodes are made of the same material, C_1 and C_2 can be written as

$$C_1 = \sqrt{n_s}e^{i\theta_1}, C_2 = \sqrt{n_s}e^{i\theta_2}. \tag{1.4}$$

Substituting these in (1.3), following equations are obtained with $\varphi = \theta_2 - \theta_1$.

$$\begin{cases} i\hbar\dfrac{dn_s}{dt} - 2\hbar n_s\dfrac{d\theta_1}{dt} = 2eVn_s + 2Kn_se^{i\varphi} \\ i\hbar\dfrac{dn_s}{dt} - 2\hbar n_s\dfrac{d\theta_2}{dt} = 2Kn_se^{-i\varphi} - 2eVn_s \end{cases} \tag{1.5}$$

By separating real and imaginary parts,

$$\begin{aligned} \frac{dn_s}{dt} &= \frac{2Kn_s}{\hbar}\sin\varphi \\ \frac{d\theta_1}{dt} &= -\frac{K}{\hbar}\cos\varphi - \frac{eV}{\hbar} \\ \frac{d\theta_2}{dt} &= -\frac{K}{\hbar}\cos\varphi + \frac{eV}{\hbar} \end{aligned} \tag{1.6}$$

These lead to the following Josephson equations, the bridge between physical quantities (n_s, V) and the wave function's phase difference.

$$\begin{cases} \dfrac{dn_s}{dt} = \dfrac{2Kn_s}{\hbar}\sin\varphi \\ \dfrac{d\varphi}{dt} = \dfrac{2eV}{\hbar} = \dfrac{2\pi}{\Phi_0}V \end{cases} \tag{1.7}$$

Here, $\Phi_0 = h/2e$ is a magnetic flux quanta. It is obvious that $I_s \propto dn_s/dt$, which implies the relation between the critical current I_c and I_s under the existence of the phase difference.

$$I_s = I_c \sin\varphi \tag{1.8}$$

This is so-called **DC Josephson effect**. Using the Josephson equation and $L = V(\frac{dI_s}{dt})$, one can obtain the non-linear inductance of a Josephson junction.

$$L_s = V(I_c\cos\varphi\frac{d\varphi}{dt})^{-1} = \frac{\Phi_0}{2\pi I_c\cos\varphi} = L_c\frac{1}{\cos\varphi} \tag{1.9}$$

1.1.2 Flux-Tunability of DC SQUID

A DC SQUID, or two-junction SQUID, can be seen as two Josephson junctions connected in parallel forming a loop. To understand the operation of a SQUID, I focus on the relation between the maximum current flowing without voltage drop $I_s^{\max}$ and the total magnetic flux Φ enclosed in the SQUID loop. One can approach the phase difference of the two Josephson junctions by carrying out the line integral following the contour $\overline{12341}$ in Figure 1.1. The generalized momentum of a Cooper pair is

$$\hbar\nabla\theta = 2m\vec{v_s} + 2e\vec{A}\ , \tag{1.10}$$

where $\vec{v_s}$ is the pair velocity, which is assumed since we can regard that the integration path is far away from the edges of the material. The closed integral is given by following.

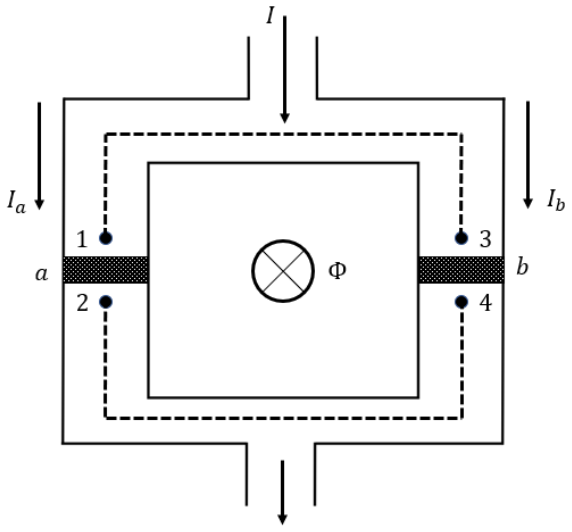

Figure 1.1: A DC SQUID with two Josephson junction a and b. Magnetic flux Φ is enclosed inside the loop.

$$\hbar\left(\int_1^3 \nabla\theta\cdot d\vec{l}+\int_4^2 \nabla\theta\cdot d\vec{l}\right)=2e\left(\int_1^3 \vec{A}\cdot d\vec{l}+\int_4^2 \vec{A}\cdot d\vec{l}\right) \tag{1.11}$$

Using the phase difference and provided that the vector potential does not have any special features near the junctions,

$$\theta_3-\theta_1+\theta_2-\theta_4=\varphi_a-\varphi_b=\frac{2e}{\hbar}\oint \vec{A}\cdot\ d\vec{l}\,. \tag{1.12}$$

By Stokes' theorem, the integral on the RHS is equivalent to the magnetic flux enclosed in the loop.

$$\varphi_a-\varphi_b=2\pi\frac{\Phi}{\Phi_0} \tag{1.13}$$

Then the current flowing through the SQUID can be represented as following by Kirchhoff's law and the result from the previous section, (1.8).

$$\begin{aligned}
I=I_a+I_b&=I_c(\sin\varphi_a+\sin\varphi_b)\\
&=2I_c\sin\left(\frac{\varphi_a+\varphi_b}{2}\right)\cos\left(\frac{(\varphi_a-\varphi_b}{2}\right)\\
&=2I_c\sin\left(\varphi_b+\frac{\varphi_a-\varphi_b}{2}\right)\cos\left(\frac{(\varphi_a-\varphi_b}{2}\right)\\
&=2I_c\cos\left(\pi\frac{\Phi}{\Phi_0}\right)\sin\left(\varphi_b+\pi\frac{\Phi}{\Phi_0}\right)
\end{aligned}$$

It turned out that the maximum dissipation-free current relies on the magnetic flux enclosed in the SQUID loop.

$$I_s^{\max}=2I_c\left|\cos\pi\frac{\Phi}{\Phi_0}\right| \tag{1.14}$$

In principle, in order to accurately estimate the magnetic flux, we should account two factors; the external flux and the screening flux created by the loop itself as a reaction to the external flux. The screening flux is quantified via so-called screening parameter.

$$\beta_L=\frac{2L_{\text{loop}I_c}}{\Phi_0} \tag{1.15}$$

Then, the total external flux through the SQUID loop is

$$\Phi=\Phi_{ext}-\frac{\beta_L}{2}\Phi_0\cos\left(\frac{\varphi_a+\varphi_b}{2}\right)\sin\left(\frac{\varphi_b-\varphi_a}{2}\right) \tag{1.16}$$

By considering a limit $\beta_L\approx 0$, the maximum dissipation-free current becomes a function of the external magnetic flux.

$$I_s^{\max}(\Phi_{\text{ext}})=2I_c\left|\cos\pi\frac{\Phi_{\text{ext}}}{\Phi_0}\right| \tag{1.17}$$

Combining this result with (1.9), a DC SQUID can be regarded as a single Josephson junction with a flux-modulated maximum supercurrent. The flux tunable inductance of the DC SQUID is given as following.

$$L_s(\Phi_{\text{ext}}) = \frac{\Phi_0}{2\pi I_s^{\max}} = \frac{\Phi_0}{4\pi I_c \left|\cos \pi \frac{\Phi_{\text{ext}}}{\Phi_0}\right|} \tag{1.18}$$

This is one of the most important features of the DC SQUID, allowing it to be used for a non-linear flux tunable inductance for the flux-tuning JPA.

1.2 Theoretical Framework

Based on the previous discussions about the DC SQUID, I now offer a structure of flux-driven JPA. While the operations of a JPA include complicated processes, which are described by the input-output theory and quantized circuit theory, I want to approach the JPA from a fundamental perspective. A JPA can be seen as an RLC oscillator occupied by quantized photons, even though the two objects are not compatible. Therefore, it is possible to glimpse how the JPA works through the basic properties of a damping oscillator, a lumped element RLC circuit, and a quantized harmonic oscillator in the interaction picture.

1.2.1 Flux-Driven Josephson Parametric Amplifier

A flux-driven Josephson parametric amplifier (usually just refereed as JPA) is basically a coplanar quarter-wavelength waveguide terminated by a DC SQUID [5], as shown in Figure 1.2. The JPA is basically an one-port device, which requires a circulator at the input in order to seprate the input and output. A JPA chip (size of few millimeters) is installed on a printed circuit board (PCB) normally, and the chip is mounted in a holder around which a coil is wound. The coil provides magnetic flux to the DC SQUID inside the JPA through DC current (usually this current is referred as flux bias). The DC current adjusts the tunable inductance of the DC SQUID, which governs the resonance frequency of the entire JPA. Since the resonance frequency on a (R)LC circuit is proportional to $1/\sqrt{L}$, the resonance frequency of the JPA has a periodicity associated with the magnetic flux quanta. The resonant frequency as a function of coil current is shown in Figure 1.3.

An AC line called pump is coupled with the DC SQUID. The pump line offers fluctuations to the magnetic flux going through the DC SQUID, and therefore modulates the resonance frequency of the JPA (depicted in Figure 1.3). The JPA amplifies the signal power via this pumping. This process is called parametric amplification or parametric pumping, because the amplification is achieved by changing a parameter (in this case, the inductance of the DC SQUID).

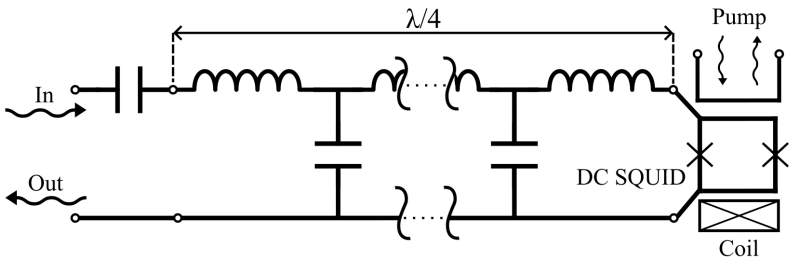

Figure 1.2: Schematic of a flux-driven JPA. The X signs on the DC SQUID stand for Josephson junctions. The coil is actually larger than the JPA chip, but is depicted in a small size for convenience. A coupling capacitor at the beginning of the waveguide limits the frequency range of the input signal. Off-resonance signals cannot go through the JPA and just reflected at the coupling capacitor.

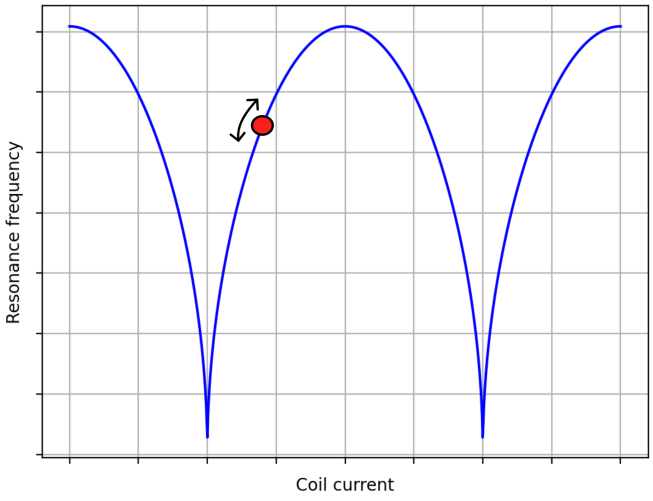

Figure 1.3: The resonance frequency of the JPA as function of DC current flowing through the coil, that is, external magnetic flux. The resonance frequency is fixed at a point like a red dot by applying a constant coil current. The AC pump line providing time-varying magnetic flux modulates the fixed resonance by a little amount.

1.2.2 Phase Response

One of the important features of a JPA is the phase response. After absorbed by the JPA, signal suffers a characteristic phase change according to the coupling condition. Since the microwave range wavelength is much longer than the size of a JPA chip, a quarter-wavelength resonator of the JPA can be regarded as a lumped element RLC circuit closed to the resonance (Figure 1.4).

The photon loss rates of the resonator is divided into two parts; the internal loss and external loss. The photons dissipated inside the resonator are described by the internal loss rate γ_i, while the photons leaving the resonator via the coupling capacitance are accounted by the external loss rate γ_e.

$$\gamma_i = \frac{\omega_0}{2Q_i}, \quad \gamma_e = \frac{\omega_0}{2Q_e} \tag{1.19}$$

f_0 is the resonance frequency of the resonator, Q_i and Q_e are internal and external quality factor, respectively.

$$Q_i = \omega_0 R(C + C_c), \quad Q_e = \frac{C + C_c}{Z_0 C_c^2 \omega_0} \tag{1.20}$$

Z_0 stands for the impedance of the transmission line connected to the resonator (usually 50Ω). The reflection coefficient Γ should be identified in order to observe the phase change of the input and output.

$$\Gamma = \frac{Z_R - Z_0}{Z_R + Z_0} \tag{1.21}$$

Z_R is the impedance of the resonator, which is expressed as

$$Z_R = \frac{1}{i\omega C_c} + \left(\frac{1}{R} + \frac{1}{i\omega L} + i\omega C\right)^{-1} = \frac{1 - \omega^2 L(C + C_c) + i\omega L/R}{i\omega C_c(1 - \omega^2 LC) - \omega^2 C_c L/R}. \tag{1.22}$$

After a set of manipulations, the reflection coefficient is obtained.

$$\Gamma = \frac{1 - \omega^2 L(C + C_c) + i\omega L/R - Z_0 i\omega C_c(1 - \omega^2 LC) + Z_0 \omega^2 CL/R}{1 - \omega^2 L(C + C_c) + i\omega L/R + Z_0 i\omega C_c(1 - \omega^2 LC) - Z_0 \omega^2 CL/R} \tag{1.23}$$

A useful representation can be obtained with an approximation $R \gg Z_0$ [6]. Combining with $\omega_0 = 1/\sqrt{L(C + C_c)}$,

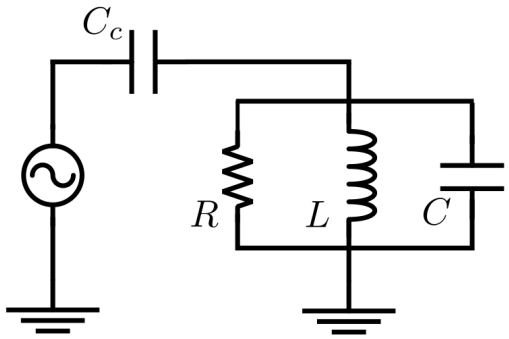

Figure 1.4: Diagram of a lumped-element RLC circuit with a coupling capacitance C_c.

the reflection coefficient is written as

$$\begin{aligned}\Gamma &= \frac{1-(\omega/\omega_0)^2+i\omega(L/R-Z_0C_c(1-\omega^2LC))}{1-(\omega/\omega_0)^2+i\omega(L/R+Z_0C_c(1-\omega^2LC))} \\ &= \frac{1-(\omega/\omega_0)^2+i(\omega/\omega_0)\left(\dfrac{\omega_0L(C+C_c)}{Q_i}+\dfrac{(\omega/\omega_0)^2C-(C+C_c)}{C_cQ_e}\right)}{1-(\omega/\omega_0)^2+i(\omega/\omega_0)\left(\dfrac{\omega_0L(C+C_c)}{Q_i}-\dfrac{(\omega/\omega_0)^2C-(C+C_c)}{C_cQ_e}\right)}\end{aligned} \tag{1.24}$$

To simplify above, $\kappa = C_c/(C+C_c) \ll 1$ is introduced, which forces $\kappa Q_i,\ \kappa Q_e \gg 1$. Also, only the vicinity of the resonance is observed: $\omega = \omega_0 + \delta\omega$ is used to make a Taylor expansion of $(\omega/\omega_0)^2$.

$$\begin{aligned}\Gamma &= \frac{-2\delta\omega/\omega_0+i(1+\delta\omega/\omega_0)\left(\dfrac{1}{Q_i}-\dfrac{1-(1-\kappa)(1+2\delta\omega/\omega_0)}{\kappa Q_e}\right)}{-2\delta\omega/\omega_0+i(1+\delta\omega/\omega_0)\left(\dfrac{1}{Q_i}+\dfrac{1-(1-\kappa)(1+2\delta\omega/\omega_0)}{\kappa Q_e}\right)} \\ &\approx \frac{\delta\omega-i(\omega_0/2Q_i-\omega_0/2Q_e)}{\delta\omega-i(\omega_0/2Q_i+\omega_0/2Q_e)} = \frac{\delta f-i(\gamma_i-\gamma_e)}{\delta f-i(\gamma_i+\gamma_e)}\end{aligned} \tag{1.25}$$

Now the magnitude of the reflection coefficient is easily obtained by $|\Gamma| = \sqrt{\mathrm{Re}(\Gamma)^2+\mathrm{Im}(\Gamma)^2}$. The phase response, which is the argument of the reflection coefficient is

$$\arg(\Gamma) = \arctan\left(\frac{2\gamma_e\delta f}{\delta f^2+(\gamma_i^2-\gamma_e^2)}\right). \tag{1.26}$$

The most useful condition is the overcoupled state $Q_i > Q_e$, where the photons inside the resonator almost leave the resonator through the coupling capacitor and not are dissipated inside it. The phase response of an overcoupled state is illustrated in Figure 1.5.

This phase response is important in experiments. The reflection coefficient is called S11 especially for the S-parameters of a vector network analyzer (VNA). The resonant frequency of JPAs are detected by the most drastic decrease of the reflection phase of S11.

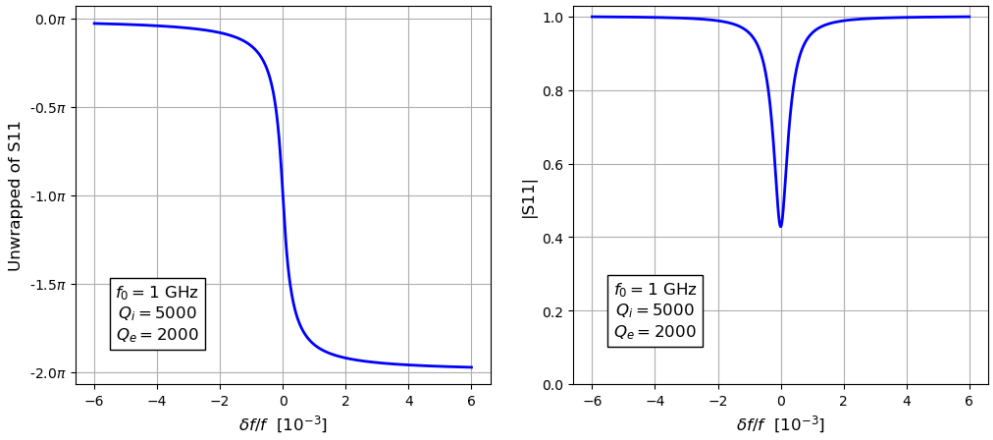

Figure 1.5: Examples of the magnitude and phase response of S11 in the overcoupled state with some parameters.

1.2.3 Noise Limit of a Phase-Insensitive Amplifier

A classical time-varying voltage signal around frequency ω can be decomposed into two orthogonal Fourier components.

$$V(t) \propto [X_1(t)\cos(\omega t) + X_2(t)\sin(\omega t)] \tag{1.27}$$

The time varying coefficient $X_1(t)$ and $X_2(t)$ are called the quadratures of the signal. Using time-varying constants a and a^*, the expression above can be converted into

$$V(t) \propto [ae^{-i\omega t} + a^* e^{i\omega t}]. \tag{1.28}$$

It is easy to find the following relations.

$$X_1 = \frac{1}{2}(a + a^*), \quad X_2 = \frac{1}{2i}(a - a^*) \tag{1.29}$$

Now introduce the analogy of the quantized harmonic oscillator; a and a^* become the quantum mechanical operators a and $a^\dagger$, which follow the bosonic commutation relation $[a,\ a^\dagger] = 1$. Then,

$$[X_1,\ X_2] = \frac{1}{2i}[a^\dagger,\ a] = \frac{i}{2}. \tag{1.30}$$

It implies that X_1 and X_2 are conjugate observables (note that their operators are hermitian) ruled by the Heisenberg's uncertainty principle. This is where the quantum noise limit comes from.

An amplifier is called phase-insensitive when the amplifier adds equal amount of noise to both quadratures [7]. Now suppose a bosonic phase-insensitive amplifier, whose input and output both from bosonic modes. Let the output operators be b and $b^\dagger$. Then, with the photon number gain G, following is an attractive assumption (note that $\sqrt{G}$ is used as the number of photons is described by $a^\dagger a$).

$$b = \sqrt{G}a, \quad b^\dagger = \sqrt{G}a^\dagger \tag{1.31}$$

However, it fails because $[b,\ b^\dagger] = 1$ does not hold. It is forced to add an additional operator, F. Turning to the quadrature expression, the amplified output quadratures can be written as

$$Y_1 = \sqrt{G_1}X_1 + F_1, \quad Y_2 = \sqrt{G_2}X_2 + F_2. \tag{1.32}$$

Providing the condition $[Y_1,\ Y_2] = [X_1,\ X_2] = i/2$ leads to following, with an assumption $[X_i,\ F_j] = 0$.

$$[F_1,\ F_2] = \frac{i}{2}[1 - \sqrt{G_1}\sqrt{G_2}]. \tag{1.33}$$

The uncertainty principle $\Delta A \Delta B \geq |[A,\ B]|/2$ yields

$$\Delta F_1^2 \Delta F_2^2 \geq \frac{G_1 G_2}{16}\left(1 - \frac{1}{\sqrt{G_1}\sqrt{G_2}}\right)^2. \tag{1.34}$$

Assume $G_1 = G_2 = G$ for simplicity. Since the phase-preserving amplifier add equal amount of noise to both quadratures, $\Delta F_1^2 = \Delta F_2^2$. Therefore, the number of added photons is

$$N_{\text{add}} = \frac{\Delta F_1^2}{G} + \frac{\Delta F_2^2}{G} = \frac{1}{2}\left(1 - \frac{1}{G}\right) \geq \frac{1}{2}. \tag{1.35}$$

This is the Haus-Caves theorem for the phase-preserving amplifier. The number of added noise photons cannot go below 1/2. This is called the standard quantum limit (SQL) or half quanta noise.

Note that 1.33 with $G_1 = G_2 = G$ can be interpreted by introducing a set of quadrature operators I_1 and I_2, satisfying $[I_1,\ I_2] = i/2$.

$$F_1 = \sqrt{G-1}I_1, \quad F_2 = \sqrt{G-1}I_2 \tag{1.36}$$

It can be regarded that an additional input mode is amplified with the gain $G - 1$. This is called the idler mode, which is an unavoidable result of the bosonic phase-insensitive amplification. In the phase-insensitive amplificaiton, the signal is amplified with additional noise which is carried by the idler mode. This is because the idler does not have any information related to the signal as assumed ($[X_i,\ F_j] = 0$). The noisy contribution of the idler mode is able to be removed when the signal bandwidth is sufficiently large to cover the idler mode [8] or in the quantum squeezing [9] of a phase-sensitive amplification.

1.2.4 Parametric Amplification

Parametric amplification, or parametric oscillation occurs in open systems, where an external effect causes a time variation of the parameters of the system. In a JPA, the signal is amplified only after the pump is applied, which is usually referred as JPA ON. The pump modulates the inductance of the SQUID and derives the parametric amplification. When an external DC magnetic flux is applied, the critical current of the DC SQUID linearly depends on the small AC flux variation. In 1.14, the total magnetic flux Φ is divided into the DC and AC parts. With $\pi\Phi_{DC}/\Phi_0 = \phi_d$ and $\pi\Phi_{AC}/\Phi_0 = \phi_a$,

$$I_s^{\max}(\Phi_{AC}) = 2I_c\left|\cos\pi\frac{(\Phi_{DC}+\Phi_{AC})}{\Phi_0}\right| = 2I_c|\cos\phi_d\cos\phi_a - \sin\phi_d\sin\phi_a| \approx 2I_c\left|\cos\phi_d - \sin\phi_d\left(\pi\frac{\Phi_{AC}}{\Phi_0}\right)\right| \tag{1.37}$$

Note that ϕ_d is a constant as it accounts for the DC flux, and small Φ_{AC} approximation is used at the last step. Then the inductance of the DC SQUID becomes

$$L_s(\Phi_{AC}) = \frac{\Phi_0}{2\pi I_s^{\max}} \approx \frac{\Phi_0}{4\pi I_c}\cos\phi_d{}^{-1}\left(1 + \pi\tan\phi_d\frac{\Phi_{AC}}{\Phi_0}\right) \tag{1.38}$$

This linear dependency allows the three-wave mixing, where the energy of pump photons is transferred into the signal and idler photons. The three-wave mixing can be roughly described by the scattering of photons in 3 different modes; the signal, idler, and pump.

$$\omega_P = \omega_S + \omega_I \tag{1.39}$$

A quantized harmonic oscillator coupled with external interactions is one of the effective approximations describing the three-wave mixing in the JPA.

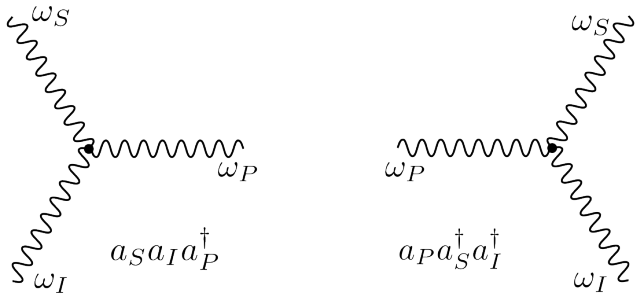

Figure 1.6: Feynman diagrams of the two kinds of interactions in the parametric pumping; creation of a pump photon from signal and idler photons (left) and annihilation of a pump photon into signal and idler photons (right).

Assuming the two scattering processes among photons as depicted in Figure 1.6, the hamiltonian of the harmonic oscillator a can be written as [10]

$$\mathcal{H} = \hbar(\omega_S a_S^\dagger a_S + \omega_I a_I^\dagger a_I + \omega_P a_P^\dagger a_p) + i\hbar\eta(a_S^\dagger a_I^\dagger a_p - a_S a_I a_P^\dagger). \tag{1.40}$$

η is a real and positive coupling constant. It shows that the harmonic oscillator is occupied with three different kinds of photons and has coupling with the scattering processes. The JPA acts as a linear amplifier only when the pump can be approximated into large amplitude, that is, classical mode.

$$a_p \to Ae^{-i\omega_P t} \tag{1.41}$$

A is the amplitude of the pump. Then, the degree of freedom related to the pump is reduced in the hamiltonian.

$$\mathcal{H}' = \hbar(\omega_S a_S^\dagger a_S + \omega_I a_I^\dagger a_I) + i\hbar\lambda(a_S^\dagger a_I^\dagger e^{-i\omega_P t} - a_S a_I e^{i\omega_P t}) = \mathcal{H}_0 + V \tag{1.42}$$

With $\lambda = \eta A$. By an unitary rotating frame operator $U = \exp[-i(\omega_S a_S^\dagger a_S + \omega_I a_I^\dagger a_I)t]$, the interaction picture representation of the hamiltonian can be obtained.

$$V_I = \exp[i(\omega_S a_S^\dagger a_S + \omega_I a_I^\dagger a_I)t] V \exp[-i(\omega_S a_S^\dagger a_S + \omega_I a_I^\dagger a_I)t] = i\hbar\lambda(a_S^\dagger a_I^\dagger - a_S a_I) \tag{1.43}$$

From this hamiltonian, the Heisenberg equations of motion for the signal and idler mode is obtained as

$$\begin{aligned} \frac{d}{dt}a_S &= \frac{i}{\hbar}[V_I,\ a_S] = \lambda a_I^\dagger \\ \frac{d}{dt}a_I^\dagger &= \frac{i}{\hbar}[V_I,\ a_I^\dagger] = \lambda a_S. \end{aligned} \tag{1.44}$$

The solution of this system of differential equations is

$$\begin{aligned} a_S(t) &= \cosh(\lambda t) a_S(0) + \sinh(\lambda t) a_I^\dagger(0) \\ a_I^\dagger(t) &= \cosh(\lambda t) a_I^\dagger(0) + \sinh(\lambda t) a_S(0) \end{aligned} \tag{1.45}$$

It shows that the amplitude of the signal mode increases exponentially. Note that the signal is not amplified forever but until the JPA is saturated, which is not observed in this simple model. This result can be interpreted as a transformation between the input (a) and output (b) modes of the amplifier [11]. With the saturation parameter $\lambda t_{\text{sat}} = r$,

$$\begin{pmatrix} b_S \\ \\ b_I^\dagger \end{pmatrix} = \begin{pmatrix} \cosh r & \sinh r \\ \\ \sinh r & \cosh r \end{pmatrix} = \begin{pmatrix} a_S \\ \\ a_I^\dagger \end{pmatrix} \tag{1.46}$$

Note that $\cosh^2 r = \sinh^2 r + 1$ implies that the difference between the gain of the signal and idler mode is 1, as discussed in section 1.2.3.

1.2.5 Lorentzian Gain

Obtaining a rigid expression of the gain of a JPA has been done through the establishment of the input-output theory of the JPA [3]. Here, I want to show that the Lorentzian property of the gain of the JPA is not really an unique case, but a basic property of damping driven oscillators.

The eqaution of the oscillator with resonance at ω_0 is given as below, assuming a cosine pump.

$$\ddot{x}(t) + 2\gamma\dot{x}(t) + \omega_0^2 x(t) = \omega_0^2 X_0 cos(\omega t) \tag{1.47}$$

γ is a damping ratio, and $\omega_0^2 X_0$ can be interpreted as an amplitude of the pump. To solve the equation, a conventional ansatz $x(t) = x_0 \cos(\omega t - \phi)$ can be applied. After substitution the ansatz, the equation becomes

$$(\omega_0^2 - \omega^2)x_0 \cos(\omega t - \phi) - 2\gamma\omega x_0 \sin(\omega t - \phi) = \omega_0^2 X_0 \cos(\omega t). \tag{1.48}$$

By expanding sin and cos term, the equation can be divided into two groups according to the dependency on $\sin\omega t$ and $\cos\omega t$.

$$\begin{cases} (\omega_0^2 - \omega^2)x_0 \cos\phi + 2\gamma\omega x_0 \sin\phi = \omega_0^2 X_0 \\ (\omega_0^2 - \omega^2)x_0 \sin\phi - 2\gamma\omega x_0 \cos\phi = 0 \end{cases} \tag{1.49}$$

From the second equation, $\tan\phi$ value is obtained.

$$\tan\phi = \frac{2\gamma\omega}{\omega_0^2 - \omega^2} \tag{1.50}$$

Using this value, $\sin\phi$ and $\cos\phi$ values are also obtained, which provides an expression of x_0;

$$x_0 = \frac{X_0}{\sqrt{(1 - \omega^2/\omega_0^2)^2 + (2\gamma/\omega)^2}}. \tag{1.51}$$

Here, the quality factor of the oscillator is defined at $\omega = \omega_0$.

$$Q = \frac{x_0(\omega = \omega_0)}{X_0} = \frac{\omega_0}{2\gamma} \tag{1.52}$$

In order to observe the vicinity of the resonance, the same approximation as used in the phase response is used; $\delta\omega = \omega - \omega_0 \ll \omega_0$.

$$\frac{x_0}{x_0(\omega=\omega_0)} = \frac{2\gamma/\omega_0}{\sqrt{(1-\omega^2/\omega_0^2)^2 + (2\gamma/\omega)^2}} \approx \frac{2\gamma/\omega_0}{\sqrt{(2\delta\omega/\omega_0)^2 + (2\gamma/\omega_0)^2}} \tag{1.53}$$

The square of the amplitude is proportional to the energy stored in the resonant system. Therefore,

$$E \propto \frac{1}{1 + 4Q^2\delta\omega^2/\omega_0^2}. \tag{1.54}$$

This is so-called Lorentzian response. Note that it is only valid with the weak damping $Q \gg 1$, since only a single sharp frequency ω_0 is regarded as the self resonance of the oscillator [10].

As discussed, the JPA can be seen as an electric oscillator, which is mathematically equivalent to the damping oscillator. The JPA shows Lorentzian gain centered at its resonance frequency, as a response to the pump.

$$G(\omega) = \frac{G_0}{1 + 4Q^2\delta\omega^2/\omega_0^2} \tag{1.55}$$

Here, G_0 is the gain at the resonance, $\omega = \omega_0$. Even though the damping oscillator model does not explain the amplification process, It is possible to predict the gain profile of the JPA through this simple model.

References

[1] Çağlar Kutlu, Arjan F van Loo, Sergey V Uchaikin, Andrei N Matlashov, Doyu Lee, Seonjeong Oh, Jinsu Kim, Woohyun Chung, Yasunobu Nakamura, and Yannis K Semertzidis. Characterization of a flux-driven josephson parametric amplifier with near quantum-limited added noise for axion search experiments. *Superconductor Science and Technology*, 34(8):085013, 2021.

[2] Jose Aumentado. Superconducting parametric amplifiers: The state of the art in josephson parametric amplifiers. *IEEE Microwave magazine*, 21(8):45–59, 2020.

[3] Yoshihisa Yamamoto and Kouichi Semba. *Principles and Methods of Quantum Information Technologies*, volume 624. Springer, 2016.

[4] Vadim Vasil'evich Schmidt and Paul Müller. *The physics of superconductors: Introduction to fundamentals and applications*. Springer Science & Business Media, 1997.

[5] Tsuyoshi Yamamoto, K Inomata, M Watanabe, K Matsuba, T Miyazaki, William D Oliver, Yasunobu Nakamura, and JS Tsai. Flux-driven josephson parametric amplifier. *Applied Physics Letters*, 93(4), 2008.

[6] Philip Krantz. *The Josephson parametric oscillator–From microscopic studies to single-shot qubit readout*. Chalmers Tekniska Hogskola (Sweden), 2016.

[7] MJ Collett and DF Walls. Quantum limits to light amplifiers. *Physical review letters*, 61(21):2442, 1988.

[8] M Renger, S Pogorzalek, Q Chen, Y Nojiri, K Inomata, Y Nakamura, M Partanen, A Marx, R Gross, F Deppe, et al. Beyond the standard quantum limit for parametric amplification of broadband signals. *npj Quantum Information*, 7(1):160, 2021.

[9] L Zhong, EP Menzel, R Di Candia, P Eder, M Ihmig, A Baust, M Haeberlein, E Hoffmann, K Inomata, T Yamamoto, et al. Squeezing with a flux-driven josephson parametric amplifier. *New Journal of Physics*, 15 (12):125013, 2013.

[10] Aashish A Clerk, Michel H Devoret, Steven M Girvin, Florian Marquardt, and Robert J Schoelkopf. Introduction to quantum noise, measurement, and amplification. *Reviews of Modern Physics*, 82(2):1155, 2010.

[11] Manuel Angel Castellanos Beltran. *Development of a Josephson parametric amplifier for the preparation and detection of nonclassical states of microwave fields*. PhD thesis, University of Colorado at Boulder, 2010.